This is the Pre-Published Version.
X. Wu, X. Zhang, Y. Jiang, X. Huang, G. Huang, A. Usmani (2022) *Intelligent tunnel fire safety monitoring system: Framework and small-scale demonstration*, **Tunnelling and Underground Space Technology**, 104301. https://doi.org/10.1016/j.tust.2021.104301

An Intelligent Tunnel Firefighting System and Small-scale Demonstration

Xiqiang Wu[1], Xiaoning Zhang[1,2], Yishuo Jiang[3], Xinyan Huang[1,*], George G.Q. Huang[3], Asif Usmani[1]

[1]*Research Centre for Fire Safety Engineering, Department of Building Environment and Energy Engineering, The Hong Kong Polytechnic University, Hong Kong*

[2]*Research Institute for Sustainable Urban Development, The Hong Kong Polytechnic University, Hong Kong*

[3]*Department of Industrial and Manufacturing Systems Engineering, The University of Hong Kong, Hong Kong*

* Corresponding to xy.huang@polyu.edu.hk (X. Huang)

Abstract

Disastrous fire event in the confined tunnel is a fatal hazard, threatening the lives of trapped people and firefighters. Considering the rapid development of fire and the complex environment of tunnels, an accurate and timely fire identification system is in urgent need for guiding the evacuation, rescue, and firefighting actions. This study proposes an intelligent system and digital twin composed of four main components to collect, manage, process and visualize the tunnel fire information. As demonstrated in a laboratory-scale tunnel model, the AI model is trained with a large numerical database to successfully identify the fire size and location. The whole system is assessed in terms of accuracy, timeliness and robustness. The AI model attained an overall accuracy of 98% in predicting the tunnel fire scenarios. The total time delay is around 1 s from the on-site measurement of temperature to the final display of the tunnel fire scenario on a remote user interface. Moreover, the system is robust enough to predict fire, even if part of the temperature sensors is failed or destroyed by fire. The proposed intelligent system will be a valuable step for smart firefighting from the concept to practice.

Keywords: *smart firefighting; IoT system; artificial intelligence; tunnel fire prediction; fire modelling.*

Nomenclature

Symbols		CNN	convolutional neural network
D^*	characteristic fire diameter	CVV	critical ventilation velocity
l	tunnel length (m)	DBMS	database management system
Q	heat release rate (kW)	FDS	fire dynamics simulator
R^2	coefficient of determination	FN	false negative
T	temperature (K)	FP	false positive
T^*	normalized temperature	HRR	heat release rate
u	airflow velocity (m/s)	HRRPUV	heat release rate per unit volume
δx	nominal length of cell edge	IoT	Internet of Things
		LR	logistic regression
Subscripts		LSTM	long short-term memory
f	full scale	MAE	mean absolute error
m	model scale	ML	machine learning
max	maximum value	MSE	mean squared error
min	minimum value	NN	neural network
		RNN	recurrent neural network
		SFDT	Smart Firefighting Digital Twin
Abbreviations		SI	supplementary information
AI	artificial intelligence	SVM	support vector machine
ANN	artificial neural networks	TCNN	transpose convolutional neural network
API	application programming interface	TN	true negative
CCTV	closed-circuit television	TP	true positive
CFD	computational fluid dynamics	UAV	unmanned aerial vehicle

1 Introduction

Tunnel fire is a fatal hazard causing significant injuries and economic losses every year around the world. In 1987, a catastrophic tunnel fire incident in Azerbaijan, induced by an electrical fault, caused 289 deaths (Haack 2002). In 2020, a fire accident occurred in the Samae 2 Tunnel, Korea, and after the collision of dozens of tanks and trucks, the fire killed four people and injuring more than 40 others. Statistics show that there have been 161 medium to large tunnel fire accidents from 2000 to 2016 in China (Ren *et al.* 2019). Once a tunnel fire occurs, it could be fatal and cause a catastrophic economic loss (Casey 2020; Chen *et al.* 2020). The severe consequences of tunnel fire can attribute to challenging evacuation from poorly ventilated spaces with high-temperature and high-density smoke and toxic gases. Furthermore, the rapid and complex fire development inside the tunnel makes it difficult to guide the evacuation, rescue and firefighting activities. Therefore, an accurate, timely and intelligent fire identification system is in urgent need for tunnel firefighting (Beard 2009; Chen *et al.* 2020).

Fire detection relies on the collection of fire-related information, very often the smoke, heat, and flame. Today, most infrastructures are equipped with fire alarm and detection systems (e.g., smoke and

heat sensors). One widely used system is the fiber optic linear heat detection system, a line-type heat detector to detect fire based on Raman scattering (Aralt and Nilsen 2009; Liu *et al.* 2011a). The temperature profile, fire location, and fire size could also be provided (Koffmane and Hoff 2010). Although many new algorithms are proposed, conventional fire detection has a high false alarm rate due to interferences from non-fire heat and smoke sources (Baek *et al.* 2021). The closed-circuit television (CCTV) camera network has been used for tunnel fire detection in practice, and it can also determine the false alarm and monitor fire evacuation, which has been a hot research topic (Gaur *et al.* 2020; Yang *et al.* 2021). Although the conventional fire detection systems can determine the fire location in the early stage (Liu and Kim 2003; Liu *et al.* 2011b; Jevtić and Blagojević 2014), simply detecting the fire can neither tell more fire information (e.g., size, severity, development, and critical events) nor further support the coming firefighting activities. Also, the camera network is not reliable to support the coming firefighting and rescue because the fire smoke plume will quickly cover the ceiling and block the cameras from capturing the visual information of fire.

An intelligent firefighting system requires a real-time monitoring of fire development and severity and the reconstruction of temperature and smoke field, particularly the heat release rates (HRRs) and smoke movement. Moreover, such a system should be accurate, timely and robust, based on an imperfect sensor network that is partially damaged by fire and limited camera images covered by smoke. The concept of sensor-assisted data-driven firefighting has been proposed and demonstrated at the compartment and multi-room fires (Han *et al.* 2010; Cowlard *et al.* 2010; Grant *et al.* 2015; Wang *et al.* 2021), and multiple inverse modeling methods have been proposed (Jahn *et al.* 2011, 2012). Driven by the recent booming of deep learning and high-performance computing, numerous studies have proposed artificial intelligence (AI) methods for fire detection and fire risk assessment, particularly in wildland fires (Akhloufi *et al.* 2018; Sayad *et al.* 2019). Compared with conventional knowledge-based methods, one advantage of data-driven approaches is that they can automatically learn the hidden features or relationships from the available data. Massive images of smoke and flame have also been adopted to train deep learning algorithms to improve the accuracy of fire detection and reduce the rate of false alarms (Cao *et al.* 2019; Govil *et al.* 2020). Many neural networks (NNs) based algorithms have also been developed to pinpoint the wildfire location and forecast fire (Ghoreishi 2019; Hodges and Lattimer 2019; Zhai *et al.* 2020).

AI methods have also been applied in fire detection and forecast in different infrastructures and support the fire engineering design. For example, machine learning techniques have been proposed to train the historical experimental data and determine the critical conditions for flashover (Dexters *et al.* 2020). The numerical compartment-fire database formed by the simulation results of zone-model are also trained by AI (called the P-Flash model) to predict the flashover (Wang *et al.* 2021). The smoke motion inside the atrium has also been predicted by the deep-learning AI methods trained with the CFD fire database. Previously, we proposed an AI model to recognize the fire source information in tunnels (Wu *et al.* 2020), identify critical tunnel fire events (Zhang *et al.* 2021), and forecast the evolution of the fire and smoke layer (Wu *et al.* 2021), all of which had been demonstrated by the numerical fire modeling and database. So far, the capability of using AI plus sensor networks in identifying the real fire in the tunnel or other buildings for practical firefighting has not been explored.

This study proposes an intelligent system, namely Smart Firefighting Digital Twin (SFDT) for tunnels. The system comprises four main components (sensor network, data cloud, AI model, and user

interface) to collect, manage, process and visualize the tunnel fire information. It is capable of providing valuable information to help the firefighters to make decisions. The AI model, using long short-term memory (LSTM) layers, is trained with a numerical database and is validated through fire tests in the laboratory-scale tunnel model. The whole intelligent system is then assessed in terms of accuracy, timeliness, and robustness. Finally, guidelines are given for applying the current system to actual tunnels and smart firefighting activities.

2 System framework

To alleviate the potential significant injuries and losses to the trapped personnel and firefighters when a hazardous fire accident occurs in tunnels, an information system is preferably provided for the on-site firefighting actions. The AI algorithms, which have shown their capability in detecting and forecasting fire scenarios, are adopted in the current system to monitor the tunnel fires by deeply mining the available data collected from sensors. It is assumed that a sensor network, which could measure the temperature continuously during a fire, has already been installed in the tunnel before the fire incident happened. **Fig. 1** illustrates the framework of the proposed SFDT system of four key components:

1) A sensor network, which is installed in the tunnel prior to fire incidents to collect the on-site temperature data.
2) A cloud data server component, which reads the data remotely transferred from the sensor network into a server and store the data in a standard format.
3) An AI engine component, which makes use of the available measured data to give identification, forecasting and early warning on the potential fire scenarios to the firefighters in real-time.
4) A user interface, which could fetch the output of the AI engine for displaying the fire scene to operation center the and alarming firemen and commanders in a friendly mode.

Among these components, the AI engine enabling the digital twin to be automatic and smart in tackling the tunnel fire incident plays a central role. The arrows in the diagram indicate the direction of data flow and interaction between each component.

2.1 Sensor network

In the fire event, the smoke layer in tunnels hinders the visibility of CCTV cameras in monitoring the fire development. As a better alternative, sensors and devices that measure the temperature distribution, flow/ventilation velocity, and characteristic gas emissions from fire (e.g., CO and NOx) could be pre-installed inside the tunnels to provide more reliable data. For example, low-cost temperature sensors like thermocouples could be installed along with the lights and smoke detectors uniformly at the ceiling of the tunnel to swiftly monitor the temperature distribution of fire smoke layer.

The data measured by sensors can be transferred through cables or wireless methods. While considering the poor reception in a confined space and data transmission interfered by fires and heavy smoke, a wired connection along with the existing power cables and fire alarm wired that are buried in walls would be a preferable choice. As further illustrated in **Fig. 1**, sensors can be connected through wires to the data collection controller, which could be a typical data logger device capable of converting the voltage signals into temperature by a single-chip microcomputer. The data logger should be placed in a safe location away from fire hazards and equipped with a Wi-Fi module for data transmission.

Note that deploying an extensive number of sensors would make it difficult to maintain the system, and the service life of the sensors would be cut down if the data collection frequency is set unnecessarily

high. Thus, the data collecting and exporting frequency in a magnitude of minutes is often set in existing monitoring systems (Jiang *et al.* 2020; Sharma *et al.* 2020), and the high-frequency (> 1 Hz) model can be triggered by a high-temperature or smoke detector when a fire event occurs. The optimal distance between sensors and the operating frequency of sensors could be determined through sensitivity analysis, as discussed previously (Wu *et al.* 2020).

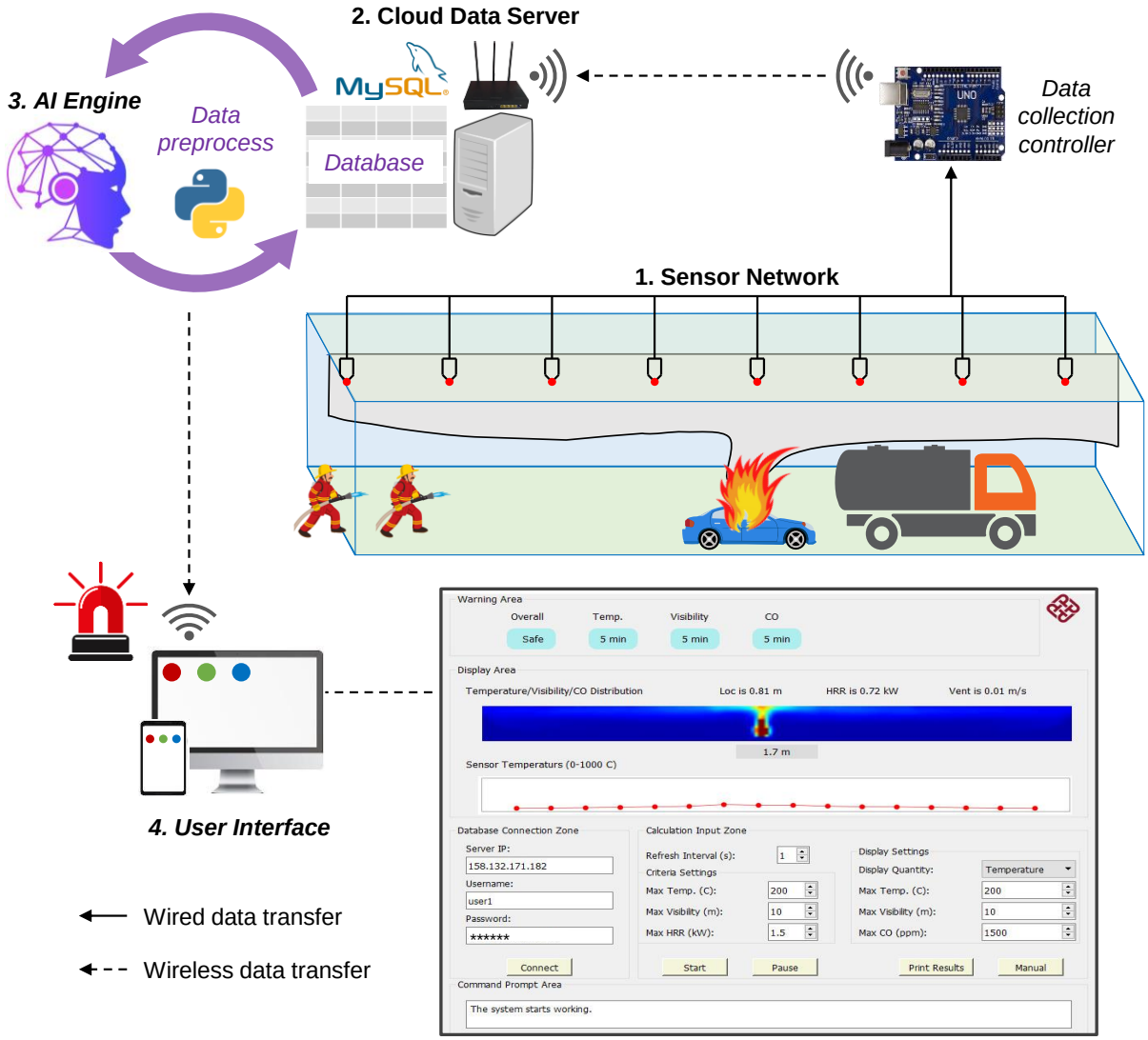

Fig. 1. The framework of the Smart Firefighting Digital Twin for monitoring the tunnel fire.

2.2 Cloud data server

The collected data is transferred through the internet to a remote cloud database, and together with the sensor network and user interface, an Internet of Things (IoT) system is formed. The cloud database can be managed by the fire services department or the emergency-response office, which are further processed by the AI engine, as shown in **Fig. 1**. Therefore, firefighters and the fire department would know the dynamic situation of the fire incident immediately before and on the way to the fire site.

The data in the database could be organized by Database Management System (DBMS) like MySQL (Zone 1997) in multiple tables connecting each other according to their relationships. Because of the lack of data standards related to fire information, the structure of the database and table needs to

be clearly defined before being filled with data. In this study, a primary database having three tables is created: a measurement table, which enables the temperature data measured by each sensor to be stored in each column; a prediction table, which is filled with the real-time predictions by the AI model; a scenario table, which stores the characteristic values and images of temperature distribution of all the simulated scenarios might happen in practice. A Python program having an application programming interface (API), i.e., MySQL Connector (Krogh *et al.* 2018), is installed on the server to connect, query and write the database.

2.3 AI engine

The AI engine on the cloud server is the key component of the intelligent system. Essentially, the AI engine behaves as a surrogate model to read the data in the database as inputs and output the predictions of fire information (e.g., fire location, size and temperature contour). The outputs will also be written into the database using the Python program include SQL command lines through the MySQL Connector API. The structure and training of the AI model are discussed in Section 3.

In practice, the collected data may be invalid, showing as 'missing,' 'out of range,' 'non-digit,' and 'burnout' due to the manufacturing flaw of a sensor, misfunction or fire damage. Although these invalid data are also stored in the database, they cannot be read directly by the AI engine. To improve the robustness of the AI engine, a filter algorithm is adopted to pre-process and interpolate the raw data in case of broken sensors.

2.4 User interface

The measured temperature and predicted results are visualized on a user interface in the computer or mobile phone screen to facilitate decision-making on firefighting. The user interface has four essential function areas: setting area, display area, warning area and command prompt area (**Fig. 1**). The setting area is composed of a connecting zone and an input zone. The IP address of the server, username, password, and name of the database need to be specified. Then the user interface could connect to the target database on the remote server with the input information. The input zone is to set the values of parameters for the AI engine, including the update interval of its output, the quantity to be output and the criterion for critical events. The display area serves as a *Smart Firefighting Digital Twin* container, where the predicted fire scene inside the tunnel could be rendered in real-time.

The operations of the start and pause of the prediction can be made to visualize the results. The changes of the input will be displayed in the command prompt area. The general dimensions of the tunnel, the temperature measured by sensors, the prediction of the fire source and the temperature distribution in the tunnel will be shown in the display area. The key information, i.e., the occurrence of the critical events and the corresponding occurrence time forecasted by the AI model, will be given in the waning area at the top of the interface. The first block in the warning area shows the occurrence of a critical event, and it will turn from green to red of the critical event happens. The other three blocks show the forecasted occurrence time of the critical events defined on temperature, toxic gases and smoke from now on. The operation process of the user interface is explained in the Supplementary Information (SI) and illustrated in demonstrated in Video S1.

3 AI methods

3.1 Numerical simulation of tunnel fire and database

This section illustrates the details of the construction of the training database, the structure of the AI model, the training settings and the evaluation of the AI model on the training database. First and foremost, a large and reliable training database is crucial to obtaining a well-performed AI model (Wu *et al.* 2021; Zhang *et al.* 2021). The database can be constructed by experimental, numerical or mixed data. In reality, it is difficult and costly to conduct real fire tests in transportation tunnels at the service stage. To explore the feasibility of an AI model trained with numerical data in predicting real fire scenarios, a training database is formed by the simulation results of various tunnel fire scenarios in this study. To enable the features hidden in fire scenarios to be learned by the AI model, the quantity and diversity of the numerical database should be sufficiently large. This could be achieved by varying key fire parameters in the simulation.

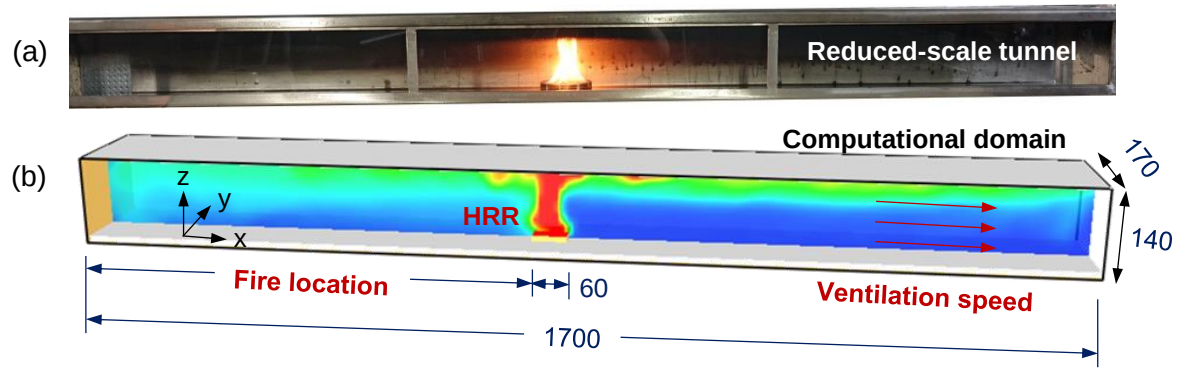

Fig. 2. Illustration of: (a) reduced-scale tunnel; and (b) numerical model (unit: mm).

Scaling is a powerful and cost-effective tool for understanding tunnel fire characteristics and smoke movement (Li *et al.* 2013). This work uses a 1:50 reduced scale tunnel model, which is 1.7 m in length, 0.14 m in height and 0.17 m in width, respectively (**Fig. 2a**). The back wall, ceiling and ground of the tunnel are made of steel plates having a thickness of 3 mm. The front wall is made of 3 mm-thick fire-retardant glass to facilitate the observation of the fire scenarios (discussed more in Section 4). For the numerical model, the boundary conditions and computational domain are set to be the same as the reduced-scale tunnel fire tests, as shown in **Fig. 3(b)**.

Fire location, fire size and ventilation condition in the tunnel are considered as the parameters, each of which are set with different values with scaling technique. Based on the Froude-number scaling analysis (Li *et al.* 2013), the HRR and flow velocity in the reduced model follows

$$\frac{Q_m}{Q_f} = \left(\frac{l_m}{l_f}\right)^{5/2} \qquad \frac{u_m}{u_f} = \left(\frac{l_m}{l_f}\right)^{1/2} \tag{1}$$

where l is the length scale, subscript "m" and "f" represent the model and full scales, respectively. Based on engineering practices and scaling rule, the values of each parameter can be determined:

- **Fire location**: The fire location is critical information to identify the fire hazard and facilitate decision-making on emergency response and fire extinguishing actions. Thus, in the simulation, the number of different values of the fire location is larger. 16 fire locations are evenly set from 0.1 m to 1.6 m to the inlet on the left-hand side of the tunnel.

- **Fire HRR**: This is the most important parameter to classify the severity of a fire, while the magnitude of HRR could vary in a large range, depending much on vehicle types. Particularly, the peak HRRs are 1.7-4.6 MW for passenger cars, 29-35 MW for buses, and 60-200 MW for tanker trucks, respectively (Ingason and Lönnermark 2012; Ingason *et al.* 2015; Hurley *et al.* 2016; Li and Ingason 2018). In this paper, five constant HRR values of 0.67 kW, 1.23 kW, 1.55 kW, 2.45 kW and 4.12 kW are assumed for the small-scale tunnel tests, corresponding to 12 MW, 27 MW, 43 MW and 78 MW in real tunnels, which covers most typical scenarios for tunnel fires. The HRR values of different fuels pans used in the current tests are calibrated in an open space. More details about the calibration are illustrated in SI.
- **Ventilation condition**: The critical ventilation velocity (CVV) is the minimum velocity to prevent the back-layering of smoke in tunnels, and its value largely depends on HRR. (Ingason *et al.* 2015). For the assumed real scale tunnel, CVV can be calculated as 2.58 m/s, when HRR is 80 MW, by using the empirical correlation proposed in (Danziger and Kennedy 1982). The ventilation speed is thus supposed between 0 m/s and 2.58 m/s to cover the variety of ventilation conditions, leading to scaled ventilations between 0 m/s and 0.36 m/s. Five velocities of 0 m/s, 0.2 m/s, 0.4 m/s, -0.2 m/s and -0.4 m/s are set for ventilation conditions. The positive (negative) values of the ventilation indicate the airflow from left (right) to right (left), as shown in **Fig. 2**. For the first-step demonstration, simple and uniform longitudinal ventilations are assumed for a tunnel.

Overall, 16 fire locations, 5 HRRs and 5 ventilation conditions produce 400 (= 16 × 5 × 5) fire scenarios. The fire scenarios are modeled with Fire Dynamics Simulator (FDS) version 6.7 (McGrattan *et al.* 2017). 3D modeling of small-scale tunnels is conducted for all the scenarios. The geometries and the surface materials of the models are set as the same as those of the scaled tunnel. The fuel representing a burning vehicle was modeled with a squared burner. The burner was located 0.01 m above the ground to mimic a vehicle fire 0.5 m off the ground in real.

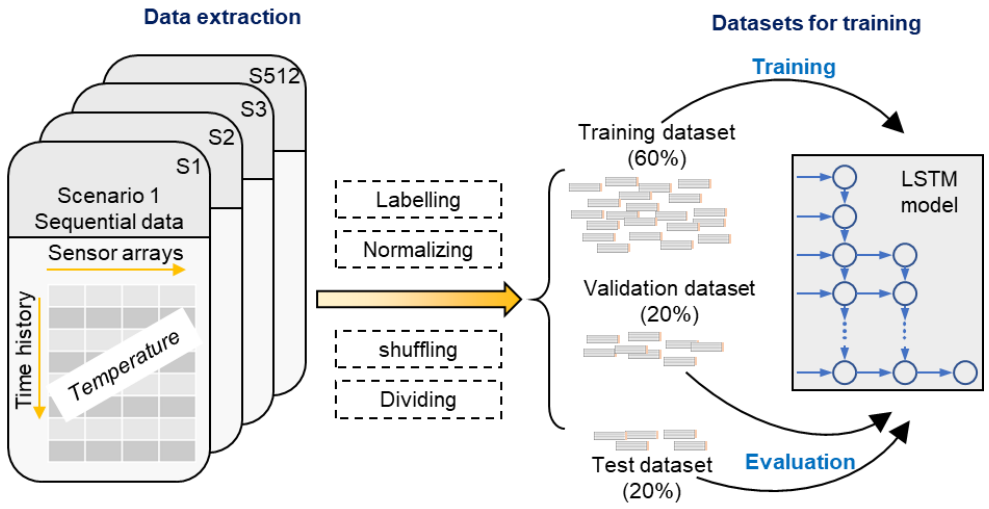

Fig. 3. Establishment of the training database.

The grid size is a key parameter for the accuracy and computational speed of modeling using FDS. The non-dimensional expression $D^*/\delta x$ is a criterion to evaluate the quality of grid resolution, where D^* is the characteristic fire diameter, and δx is the nominal length of cell edge (Mcgrattan and Mcdermott 2015). $D^*/\delta x$ is suggested to be in a range of 4-16 (Baum and Mccaffrey 1989). $D^*/\delta x$ is taken as 4 in

the current simulations. Then, the calculated maximum cell size changed from 0.012 m to 0.028 m with the increase of HRR from 0.67 kW to 4.12 kW. Thus, uniform cube cells with a size of 0.01 m are adopted in all directions. The tunnel is established in a slightly larger computational space having a total number of cells equal to 48,450. Each tunnel fire scenario was calculated for 60 s, which is long enough for all fire scenarios to reach the quasi-steady stage, where temperatures at different locations of the tunnel evolve periodically (see **Fig. S1**). Thermocouples are evenly distributed 0.01 m below the tunnel ceiling with an interval of 0.1 m to measure the gas temperature at the rate of 1 Hz. S2 gives a comprehensive comparison of the simulated and tested temperature evolvement under the same scenarios. Their coincidence demonstrates the accuracy of the CFD models.

For each simulation, temperatures measured by 16 thermocouples during a period of 60 s from the beginning of the simulation with an interval of 1 s can be recorded and stored in a data sheet. **Fig. 3** shows the flow chart to generate the database. Then, each data sheet could be cut into 8 data samples by sweeping the rows from the row of 21, since the quasi-steady stage has reached around 20 s, as illustrated in **Fig. S1**. Each sample has a temporal length of 5 s. Thus, the first three samples are the data in rows of 21-25, 26-30, and 31-35, respectively. The 8 data samples multiplying 400 scenarios form a database having 3,200 samples. With supervised learning, each sample should be labeled with an expected output. In the current paper, the output is the fire location, HRR and ventilation. Then, all the labeled samples were randomly grouped into a training dataset, a validation dataset, and a testing dataset with a ratio of 60%, 20%, and 20%, respectively. The training dataset is used for training the model, the validation dataset is used to evaluate the fitted model while training, and the test dataset is used to estimate the quality of the fitted model after training.

3.2 AI model

Deep learning algorithms have been reported to achieve satisfactory results in many areas. As a deep learning method, recurrent neural networks (RNNs) perform better at treating temporal series data than conventional ANN algorithms. LSTM model is a more advanced version of RNN models proposed by Hochreiter (Hochreiter 1997). As is named, this type of model effectively processes the input data through several gates and memorizes the useful information of the input (Bermúdez *et al.* 2017). Considering its outstanding ability in predicting with given long sequences (Greff *et al.* 2017), such as temporal series obtained from sensors, the LSTM network is adopted for the output of fire scenario characteristics, including fire location, fire size and airflow velocity. The architecture of the network is illustrated in **Fig. 4**.

Unlike some machine learning methods such as LR and decision tree, whose mechanisms can be easily interpreted (Chen 2011), the models adopted deep learning algorithms are regarded as a “black box” (Wu *et al.* 2013), and their parameters need to be verified to gain a good generality. Generally, better performance of deep learning can be achieved with more coefficients, while larger databases and training resources are unavoidable. Thus, the amount of these coefficients should be determined by balancing the training efficiency and prediction accuracy. The volume of the weights largely depends on the number of layers and hidden states in the proposed LSTM model. In addition, some functions, such as the activation function, significantly influence the performance of the model. Thus, special attention is paid to the selection of these hyperparameters.

The structure and the associated parameters of the LSTM model are determined with sensitivity studies. First, the weighted layer output can be linearly or nonlinearly transformed with activation

functions like "Linear," "Relu," "sigmoid," and "Tanh" (Arora *et al.* 2018). For the output of the end layer, suitable loss functions, options including "mean squared error (MSE)," "mean absolute error (MAE)," and "binary cross-entropy" (Sun *et al.* 2017), should be defined to be compared with the actual value. The error between the predicted and true values is then minimized by optimizer function, e.g., "Adam," "stochastic gradient descent" and "RMSprop" (Morales *et al.* 2018). After verifications, "Tanh," "mean squared error" and "Adam" is selected for the activation function, loss functions and optimizer function, respectively. The number of layers and units in each layer are then determined. The model is constructed with three layers, with the input layer having 100 states, a hidden layer having10 states and an output layer having three neurons, respectively. A dropout layer with a dropout rate of 0.1 is added to the end of the first and second layers to avoid overfitting the model. These settings are adopted for further studies. Detailed analysis of these hyperparameters is given in SI. It is noteworthy that the model structure could be further tunned with a more elaborated sensitivity study.

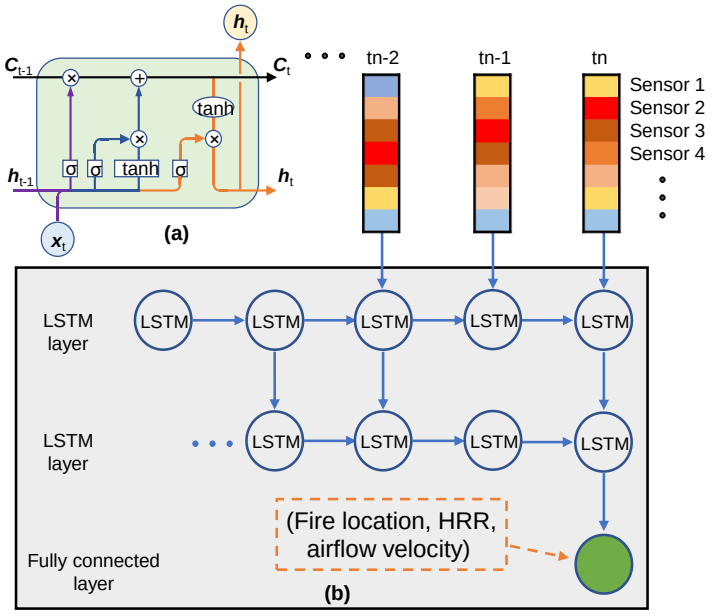

Fig. 4. The architecture of AI model: (a) basic unit of LSTM model; (b) proposed LSTM model.

The database constructed with the results of numerical simulations is used to train the proposed AI model. However, the samples should be preferably normalized before training since it is reported that the feature having a larger range would dominate the computation of similarity (Aksoy and Haralick 2001; Kumar *et al.* 2018). Thus, the labels are individually normalized to make them have the same range between 0 and 1 with a linear normalization function "MinMaxScaler" (Komer *et al.* 2014). Thus, to facilitate the recognition of the fire source severity and consider the influence of radiation heat transfer, the temperature is normalized with the function "MinMaxScaler":

$$T^* = \frac{T^4 - T_{min}^4}{T_{max}^4 - T_{min}^4} \tag{2}$$

where T_{max} [K] and T_{min} [K] are the maximum and minimum temperatures, respectively.

The normalized samples are then used to train the AI model for many epochs, which is the number of times all the training samples are used once. In each epoch, the samples are grouped into several batches, the size of which determines how many samples would be trained in one iteration of epochs.

Generally, the batch size should be determined considering the stability and the efficiency of the optimization process, and it is also limited by the physical memory of the computer or server on which an AI model is trained. In this study, 1,920 (i.e., 60% of 3,200) samples are trained in 10 batches on a server having 32 cores and 124 GB physical memories.

3.3 Performance of AI prediction

In the current study, MSE is used as the loss function to characterize how well the model behaves. Though MSE is used as a metric to evaluate the models, it cannot suggest whether a model needs to be further improved by just checking its value, e.g., it cannot be figured out whether a model gaining an MSE of 0.01 is good enough or not. As another metrics, the coefficient of determination R^2 is scale-free, meaning that it is independent of the exact differences of the predictions, and the performance of models can be directly evaluated compared with this value. Thus, R^2 has been widely adopted for the regression model (Koekkoek and Booltink 1999; Adamowski and Karapataki 2010). R^2 is also used as a criterion here for evaluating the model prediction. It should be noted that the calculated value of R^2 will not influence the optimization.

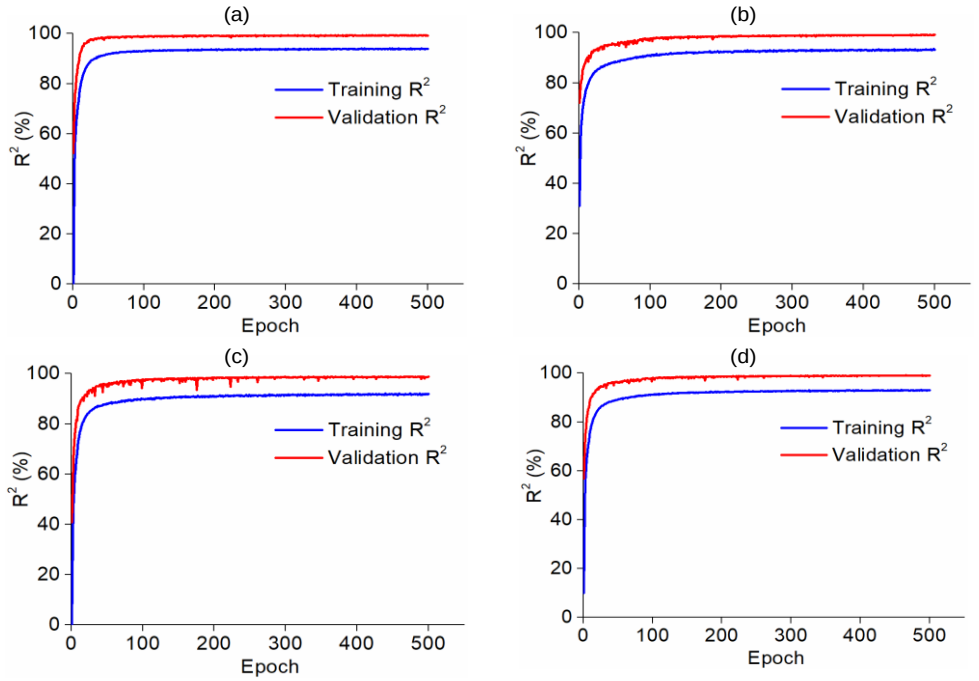

Fig. 5. The variable R^2 with (a) fire location, (b) HRR, (c) ventilation speed, and (d) the overall accuracy during the training process.

The evaluation of the established model on fire information identification is first carried out on the numerical database. **Fig. 5** shows the calculated R^2 for three fire parameters of fire location, HRR, and ventilation speed and overall performance on training and validation datasets evolving with training epochs. Compared to HRR and ventilation velocity, R^2 of fire location increases fastest with the training epochs, indicating that it is easiest to train and find the fire location inside the tunnel. From the viewpoint of tunnel fire dynamics, this is due to the more evident distinctions of temperature distribution in the tunnel caused by scenarios with fire located at different positions. Despite that, the identification of all three fire information parameters can be trained more effectively and finally converges to a high value of R^2 approaching 100%.

The training efficiency is high at the starting of training, while no apparent minimization is observed after epochs of 200 epochs, which demonstrates that the model has converged, and the pre-set training epoch number of 500 is sufficiently large. The value of R^2 on the validation dataset is comparable to that on the training dataset, meaning that the overfitting problem was not caused. A closer checking shows that R^2 is even higher on the validation dataset, which is mainly due to the setting of dropout layers. The coefficients of a certain number (dropout ratio, which is 0.1 in the current model) of units on the layers followed by a dropout layer are ignored to be updated in a training iteration, forcing the other units on the same layer to take more responsibility for the input. After then, all the units will participate in the treating of the input data on the validation dataset. As such, the model would probabilistically perform better on the validation dataset. The slight fluctuation on the training dataset, while more drastic fluctuations on the validation dataset, is a common consequence in the training of machine learning algorithms (Kavzoglu and Mather 2003; Alzubaidi *et al.* 2020).

3.4 Demonstration with CFD-modelled tunnel fire

To further check the detailed performance of the model on all the training datasets, the predictions of fire information corresponding to respective variety values are counted. The mean value and the standard deviation of each fire scenario are illustrated in **Fig. 6**. Ideally, all the data points should be aligned with the diagonal line with no divergence. However, the predicted values have shown a certain distribution around, rather than equal to the actual values. The varieties of the distribution are larger for the prediction of HRR and ventilation. As revealed in **Fig. 5**, the converging speeds of HRR and ventilation are slower than that of the fire location, indicating that the compensation effect between these two parameters is more distinct. Scenarios characterized by the combination of different values of these parameters would produce similar temperature distribution near the ceiling of the tunnel. It should be noted that despite the uncertainty in prediction, the mean value of the predictions is very close to the respective actual value, and the distribution is only confined to a small range around it.

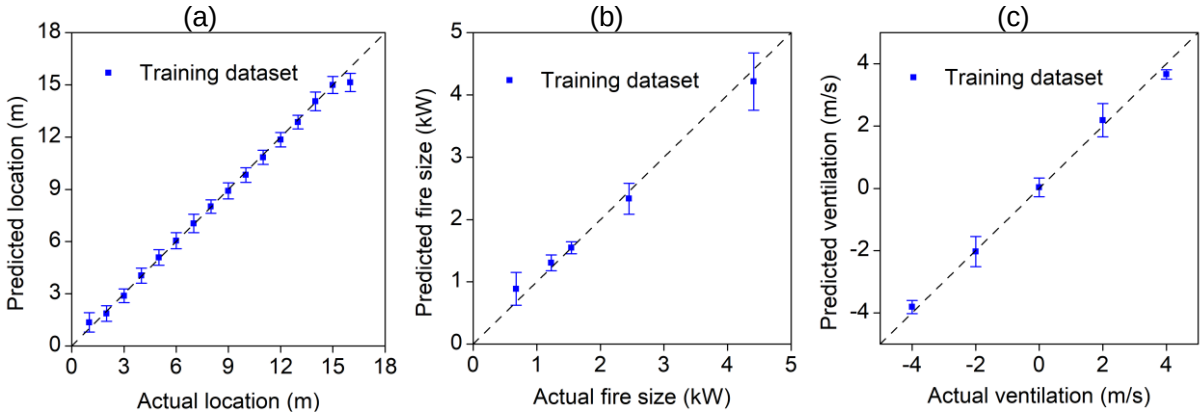

Fig. 6. Predictions by AI vs. actual fire scenario by CFD simulations, (a) fire location, (b) HRR, and (c) ventilation on the training dataset.

The fire-induced temperature distribution in the tunnel could be predicted using a complicated AI model, combing LSTM and TCNN, as proposed in our previous work (Wu *et al.* 2021). Alternatively, the temperature distribution could be directly obtained by returning the simulation results of the corresponding fire scenario predicted by the current LSTM model. After getting the prediction of the

fire location, fire size and ventilation condition, the most likely fire scenario in the numerical database could be matched. Though the temperature distribution could only be those available results simulated beforehand, the current LSTM model is much simple, intuitive and easy to be trained and explained. More importantly, the matched simulation results would be accurate enough for satisfying practical firefighting requirements if the parameters intervals between the simulated fire scenarios are small.

MSE is adopted as the evaluation function for calculating the similarity of the predicted and the stored fire scenarios. The scenario attaining the lowest value of MSE is regarded as the most likely one. It should be noted that normalization is also applied to the three predicted parameters before calculating the value of MSE. As illustrated in Section 3.2, this is to avoid the situation that a feature having a larger range would dominate the computation of similarity. Only one image showing the distribution of temperature will be shown for a simulated fire scenario. The image is the average of the last five images, that is, temporally smoothed in a period of 5 s. The averaged image hides the unnecessary details of the temperature distribution, such as the turbulent vortex structure. The last five images are selected for conversation since the fire scenario would develop into a quasi-static stage from an initially ignited fire. The averaged image is then shown on the interface to help the firefighters to recognize the areas under higher or lower temperatures more efficiently.

4 Demonstration for tunnel fire tests

4.1 Small-scale tunnel fire tests

The test setup for the small-scale tunnel fire tests is shown in **Fig. 7**. For the demonstration, the data collection controller in **Fig. 1** is represented by a datalogger and a computer, which is utilized to collect the data and send the data to the cloud server, respectively. The general dimensions and materials of the model scale tunnel are illustrated in Section 3.1. The combustible fuel adopted in the fire tests is isopropyl alcohol (also called 2-propanol, chemical formula $CH_3CHOHCH_3$) in the liquid phase. The fuel is pooled into a steel pan and the pan is then put at a designed location in the tunnel. To check the capability of the established AI model in predicting the location and size of the fire, three pans are adopted in various diameters, i.e., 38 mm, 73 mm and 90 mm, producing an HRR of 0.67 kW, 1.55 kW and 2.45 kW, respectively, according to the burning fire tests illustrated in SI. The fuel pans are put at two locations, 0.8 m and 1.2 m to the inlet on the left-hand side of the tunnel.

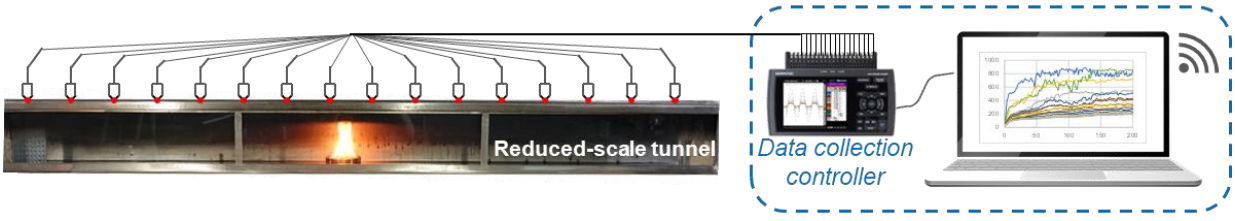

Fig. 7. Setup of the small-scale tunnel fire test.

Overall, 6 (2 × 3) tests are carried out. Each test lasts for around 7 min to get sufficient test data. Due to the restriction of the current test setup, the factor of ventilation in these tests does not vary. Instead, the airflow speed is assumed as 0 m/s because no mechanical ventilation is applied. However, since the fire sizes in the tests are small, a slight disturbance of the environmental airflow would

unexpectedly influence the ventilation condition in the small-scale tunnel. The actual airflow velocity near the fire source could be predicted by the AI model for qualitatively checking.

The temperature is measured by a datalogger GL820 produced by Graphtec Corporation. The measured temperature data are organized to form an experimental database using the similar procedure illustrated in Section 3.1 for the numerical database. Then, the experimental database is utilized to check the feasibility of predicting the information of real fire scenarios.

4.2 Performance of the trained model on real fires

Fig. 8 shows the prediction of the fire scenarios on small-scale tunnel fire tests. For comparison, the predictions on the testing dataset of the numerical data are also shown. Compared with its performance on numerical data, the trained AI model has a comparable capacity in predicting fire location and ventilation, and the deviations of the predictions on real test data are even lower. The prediction of the ventilation condition is not compared due to the missing experimental data. However, the predicted airflow velocity could be qualitatively right, considering that no mechanical ventilation is provided in the current tests and the predicted ventilation is around 0 m/s, as shown in **Fig. 8(c)**.

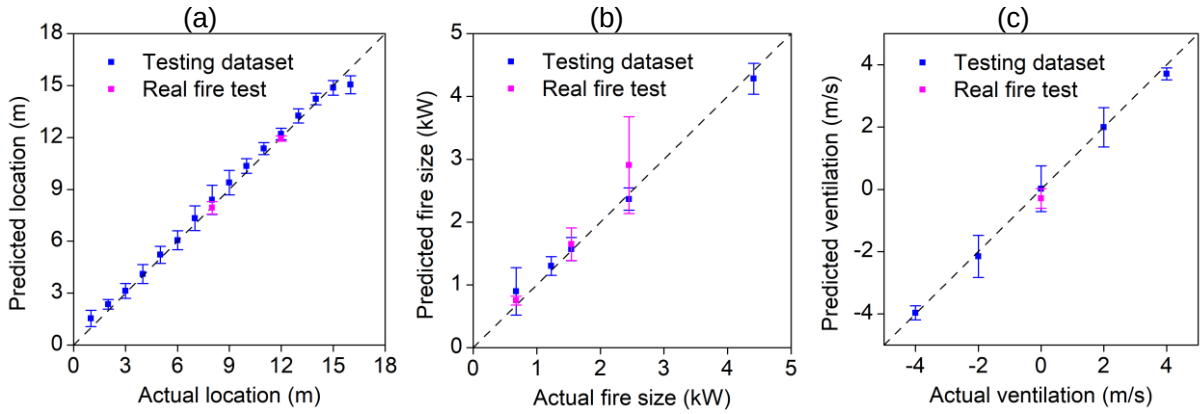

Fig. 8. Predictions of: (a) fire location; (b) HRR; and (c) ventilation on testing dataset vs. real fire test data.

The prediction of fire size on real test data is relatively poor with a larger deviation, especially for the case where HRR is 2.45 kW. To further check the reason for this divergence, the temperature evolvement in the tunnel at different locations for the simulations and real fire tests are compared at both locations of 0.8 m and 1.2 m when fire size is 2.45 kW. As shown in **Figs. 9(a)** and **(b)**, as expected, the highest temperature (red lines) occurs right above the burner at the location of 0.8 m. Both the tested and simulated highest temperatures are fluctuating around the same value near 800 °C, which indicates the deviation is not brought in by the highest temperature.

The temperatures recorded by the other thermocouples are then compared. For clarity, only the temperatures measured by the adjacent thermocouples (locations at 0.7 m and 0.9 m) are displayed. As shown, the simulated temperatures are almost fluctuating around a fixed value near 500 °C while the tested temperatures evolve with an increasing trend. Initially, the mean value of the tested temperatures increases from 440 °C to 550 °C at the time near 200 s after ignition. This lower temperature fed into the AI model produces a lower prediction of the fire size, as shown in **Fig. 9(c).** Later, the tested temperatures continue to increase and then go down due to the burnout of the combustible fuel. Accordingly, the higher temperature results in a prediction of larger fire sizes.

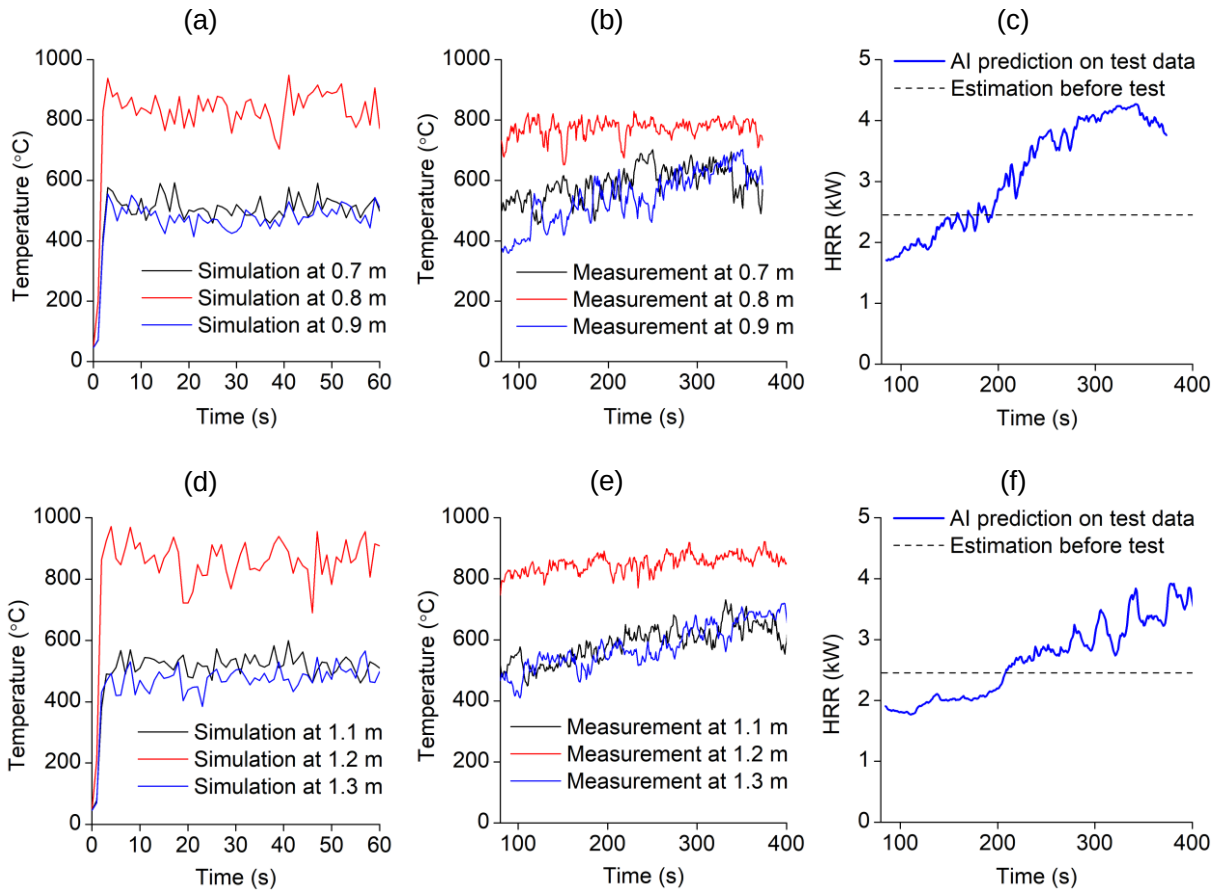

Fig. 9. Comparison of the simulated temperature evolvement (left), tested temperature evolvement (middle), and AI predictions of HRR (right): (a-c) show the case where HRR is 2.45 kW and the fire is located at 0.8 m; and (d-f) show the case where HRR is 2.45 kW and the fire is located at 1.2 m.

The similar trend of the prediction based on the tested data and the comparable cut-off point (550 °C in tests compared with 500 °C in simulation) demonstrate that the divergence of the prediction is mainly due to the difference between simulated and tested temperature evolvements, instead of the capacity of the trained AI model. This increasing trend of the temperature is mainly due to the accelerating burning of fuel. With time evolution, the inner surface of the tunnel becomes extremely high, emitting high radiation back to the fuel pan, as shown in **Fig. 7**. The heated fuel releases at a higher rate compared with the case where the fuel is burnt in an open space due to the additional radiation. Therefore, the actual HRR should have been larger than that calibrated, as illustrated in **SI**. That is, the AI model gives a more realistic estimation of the fire size in the tunnel. A similar relationship between the tested temperature and the predicted HRR is also observed in the scenarios where the fire is located at 1.2 m, and the HRR is 2.45 kW, as shown in **Fig. 9(d-f)**. With the increase of the average value of the tested temperature from 500 to 550 °C at around 200 s, the predicted HRR increases from 1.8 kW to 2.4 kW.

4.3 Pattern recognition on tunnel fire scenarios

To display the temporospatial distribution of the temperature on the user interface, the fire scenario should be recognized. Recognition is done by calculating the similarity of MSE, as illustrated in Section 3.4, between the predicted fire scenario and the available ones. All the available scenarios stored in the database constituted a scenario matrix (**Fig. 10**) having three dimensions, fire location from 0.1 m to

1.6 m along the tunnel, fire size from 0.67 kW to 4.12 kW and ventilation from -0.4 m/s (direction from right to left) to 0.4 m/s (direction from left to right).

To further analyze the predicting mechanism, the input of the AI model, i.e., the measured temperature at various locations and the simulated temperature distributions at the end of the simulation at a quasi-steady state, are compared. As shown in **Fig. 10**, the temperature of the recognized scenario and the temperature produced by its most similar scenarios, the adjacent scenarios in all the dimensions of the scenario matrix, are selected for comparison.

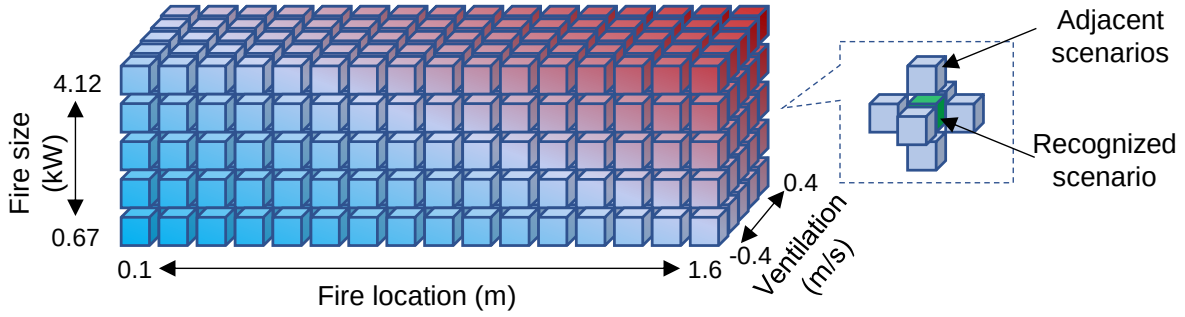

Fig. 10. The evolvement of the ventilation condition predicted by the AI model.

Fig. 11 illustrates the comparisons for cases where the fire is located at different positions and is burned at different HRRs. However, it is not easy to distinguish the fire size from their corresponding temperature distributions. The maximum temperature for cases having an HRR of 1.23 kW, 1.55 kW, and 2.45 kW is almost the same as 800 °C, rather than increasing with the increase of HRR as tested and analyzed by previous studies (Li *et al.* 2011; Li and Ingason 2012). This is because the fire sizes are so large that the fire flame impinges the ceiling of the tunnel, and the maximum temperature is the flame temperature. Thus, their main difference lies in their respective distribution instead of the maximum temperature. The higher the HRR of fire is, the "fatter" the distribution shape will be. It is also worth noting that the tested temperature is more coincident with that of the simulated fire scenario having an HRR of 2.45 kW at the neighboring points of 0.7 m and 0.9 m. While at locations far from the fire source, tested temperatures are closer to data points of the fire scenario (HRR of 1.55 kW). Finally, the tested scenario is correctly identified to have an HRR of 1.55 kW (**Fig. 11a**). This does reveal that the recognition of the AI model on fire size is not simply dependent on the maximum temperature or the temperatures near the fire source. Instead, a more complicated mechanism considering the temperature distribution is developed by the AI model. A similar phenomenon is observed on the fire scenarios having a higher HRR of 2.45 kW (**Fig. 11b**) and the fire scenario where the fire is located at 1.2 m (**Fig. 11c**)

After the fire scenario is recognized, the simulated fire scene representing by the value of the heat release rate per unit volume (HRRPUV) and the temperature distribution can be fetched from the corresponding fire scenario simulations stored in the numerical database. As shown on the left part of **Fig. 11**, the recognized fire scenes are much like those of the fire experiments. The fetched image of the temperature distribution is regarded as a Smart Firefighting Digital Twin of the real small-scale tunnel. The digital twin is then displayed on the user interface in real-time for reference.

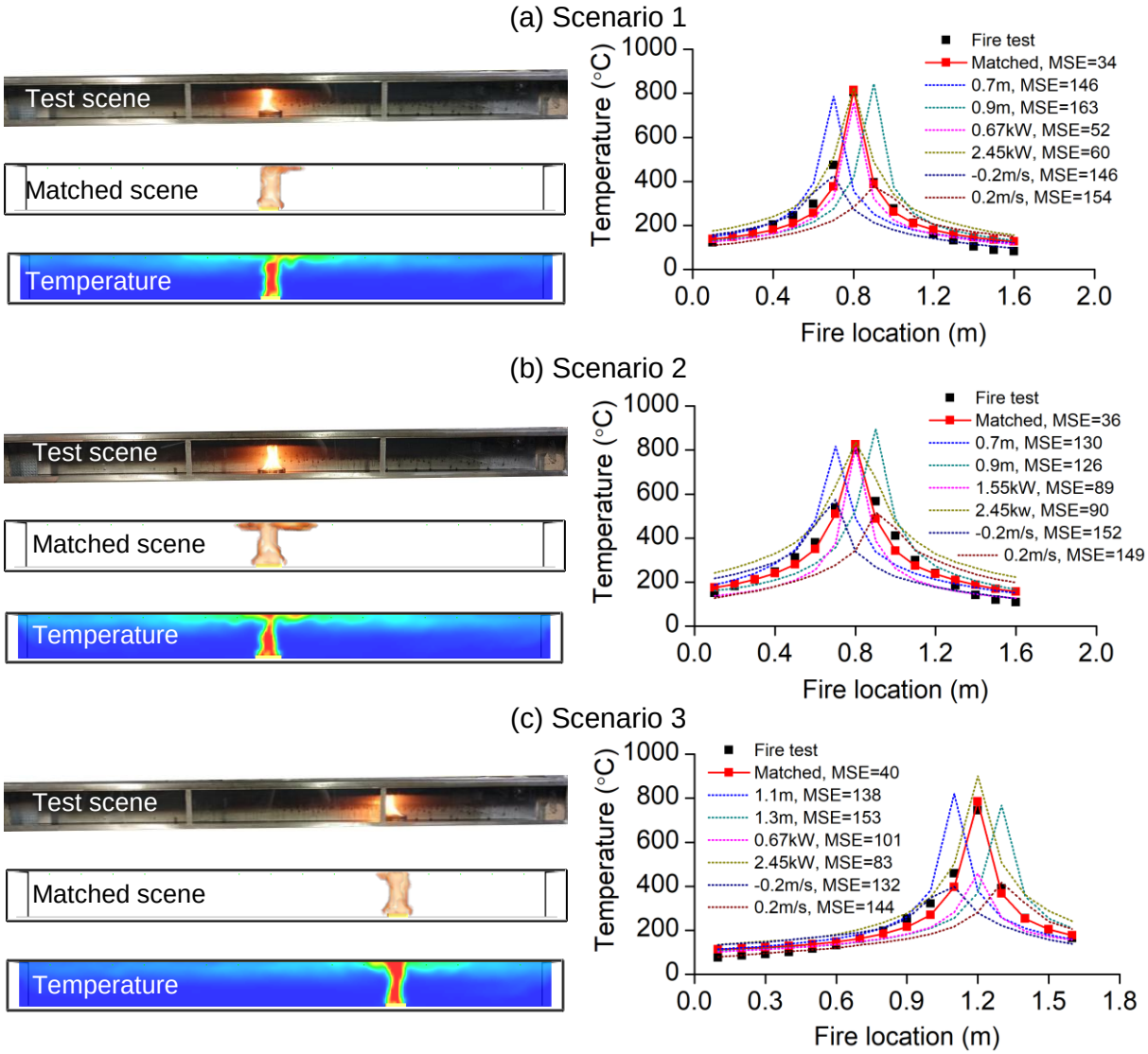

Fig. 11. Comparison of the test and matched fire scenes (left) and temperature profiles (right), where the fire location and the fire size in terms of HRR are: (a) 0.8 m and 1.55 kW; (b) 0.8 m and 2.45 kW; and (c) 1.2 m and 1.55 kW.

5 System assessment and prospective

5.1 Assessment of the whole system

Various conventional types of systems have been applied for detecting the fire location or fire size. However, they may not provide more information, such as the ventilation condition, spatially varied temperature distribution, or the occurrence of critical events, which are considered significant for firefighters. The proposed Smart Firefighting Digital Twin (SFDT) in this paper performs outstandingly in the following cases.

1) In the tunnel fire scenarios involving smoke ventilation strategies, identifying the fire source and fire severity would be challenging and inaccurate as the temperature distribution is significantly influenced by the ventilation. The proposed system can give good predictions because it has already been trained with those complicated scenarios influenced by ventilation.
2) In the fire evacuation process, the user interface of the proposed system could directly display the

temperature distribution contour, which indicates the safe and dangerous areas. Then, the emergency services will know the actual performance of the ventilation system and the efficiency of exhausting hot smokes, and then, guide the trapped personnel to evacuate to safe areas.

3) The proposed system enables the commanders and firefighters to know the fire history and current scenarios immediately once the fire incident happens. Thus, they will be better prepared and plan the firefighting and rescue strategies before arriving fire sites.
4) The early warning of critical fire events is required. The proposed system could remind the firefighters in the fire scence of possible critical events, such as backlayering and hazardous fire zones, which would alleviate the potential injuries or deaths of firefighters.

The assessment of the system is then conducted on mainly three aspects: accuracy, timeliness, and robustness. The prediction accuracies on fire information and the occurrence of the critical event have been evaluated in Sections 4.2 and 4.3.

Time Delay. Apart from the accuracy, the rapid emission of hot smoke and toxic gases during a tunnel fire makes timely identification of the fire characteristics of critical importance for guiding firefighting and rescue operations and mitigating infrastructure damage and other losses (Han and Lee 2009; Li and Liu 2020). However, certain time delays would be unavoidably necessary for the tasks, including temperature measurement by thermocouples, data transmission to datalogger, data uploading from local terminal to server, AI prediction and retrieving data from server to local user interface. The thermocouples used in the current tests are type K thermocouple extension wires with a wire diameter of 0.2 mm. The response time, defined as the time required to reach 63.2% of an instantaneous temperature change, is around 0.1 s, according to the technical specification. The type of the datalogger is GL820 produced by Graphtec Corporation. The response time of the data logger can be ignored as it is claimed to record the data and display the curves in real-time.

The time delay caused by the thermocouple and the datalogger can hardly be observed during the tests. The time delay due to all the other tasks from the local data uploading to interface displaying can be recorded by program, which is around 0.9 s based on the measurements. Thus, the time needed from the on-site measurement of temperature to displaying the predictions on a remote user interface is around 1 s in total. The fire source information and the corresponding fire scenario can be shown almost simultaneously with the real fire in the small-scale tunnel.

Another 5 s would be needed to enable the AI model to produce an accurate prediction because the current algorithm is fed by data collected within the last 5 s to remove the unnecessary noises. This longer delay is more obviously in a complex scenario when the fire size and location are changing, as shown in Video S2. Even in such complicated cases, which the AI model has not seen during training, the model can still give a good estimation, indicating that the AI model has gained specific knowledge to infer fire information for new and more complex scenarios after training. It demonstrates that the proposed system is quite swift and satisfactory. The system would perform well for providing timely information to support the decision-making of practical firefighting actions. It should also be noted that the time delay is measured on a lab-scale model, and the data transmission is through Wi-Fi at our lab. Therefore, the time delay caused by the sensor measurement in real tunnels and the data transmission through the internet could be extended.

Robustness. As a digital twin based smart firefighting system, it should also be robust to the potential changes from the internal or external environment. The system should still give some

predictions even if the collected data is not as expected. For instance, the temperature cannot be collected since a thermocouple or its wire is damaged due to the flame or hot gases. In such situations, the proposed system can still work since the filter algorithm illustrated in Section 2.4 could smooth out the missing value. After checking the prediction on fire scenarios, the firefighters could set the lower and upper bounds of the image showing the temperature distribution to know which area is safer and which area is in danger. The interface also allows the firefighters to change the criteria of the critical event for some extreme scenarios. All these flexibilities are designed to adapt the system to various emergencies in practice. Video S1 shows how to operate on the user interface under these circumstances.

5.2 Further improvement of the system

The current system is robust and is capable of giving timely and accurate predictions of tunnel fire scenarios. However, the system could be upgraded into a more powerful and intelligent system, as illustrated in **Fig. 12**. The whole system consists of four layers, the fundamental sensor layer to collect data, the network layer to transmit data, the cloud layer to process the data and the application layer to provide visual information of the fire scenarios. To achieve this ultimate system, the following aspects need to be strengthened.

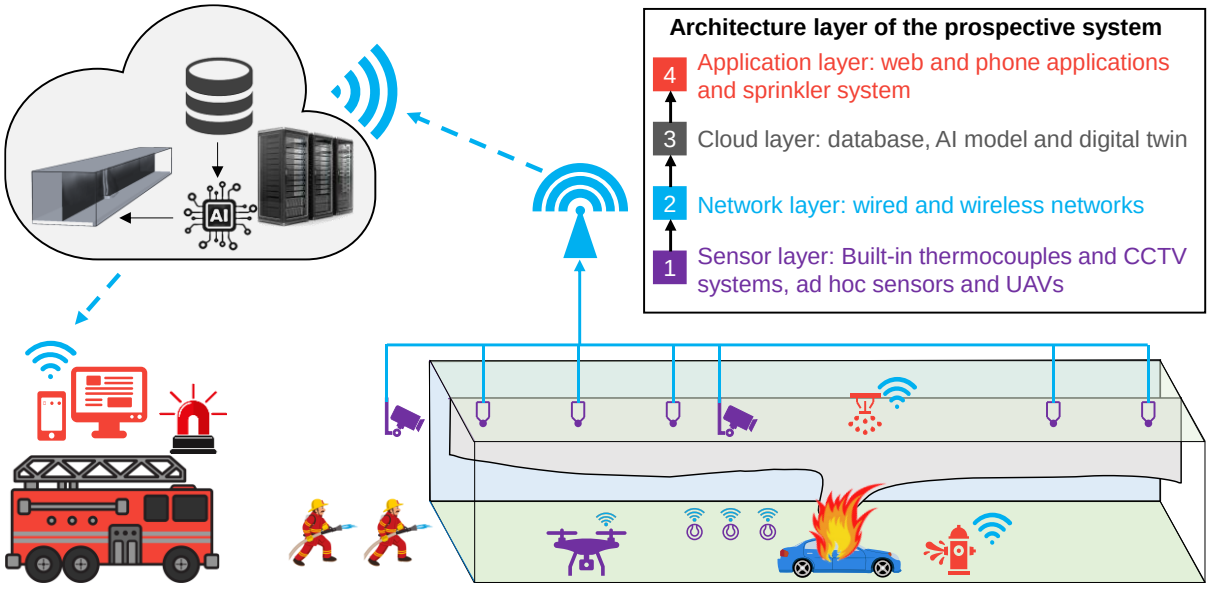

Fig. 12. Prospective intelligent tunnel firefighting system.

Data collection and transmission. Currently, only the temperature near the ceiling is measured by the thermocouples. However, more quantities, such as smoke density at certain points by the smoke sensor, visual images showing the smoke and flame by CCTV and thermal images by an infrared camera, could be collected for inference and cross-validation. The computer used in the system to send the measured data to the server can be replaced by a gateway, which is qualified to fulfill the task at a lower cost. In addition, these sensors would be wired or wireless. Wireless sensors can collect the data and then transfer the data to a gateway wirelessly, which would be a better choice for an existing tunnel since it is more convenient to install. A temporary ad-hoc network (ball-shaped sensors on the ground of the tunnel shown in **Fig. 12**) could be conveniently deployed at the location where most of the built-in sensors are destroyed by the high temperature. Other flexible sensors carried by unmanned aerial vehicles (UAVs) or firefighting robots can also be used to amend the on-site firefighting system. The

number and locations of these sensors and the data collection period should be optimized by conducting a sensitivity study, as is done in our previous works (Wu *et al.* 2020). The optimized arrangement of the sensor network will be more cost-efficient and convenient for maintenance meanwhile provide accurate predictions.

Database and AI model. The performance of the AI model much depends on the quality of the training database. A database having a big volume and lots of varieties enables the AI model to have a good generalization. The database could be improved by considering more parameters related to fire scenarios, such as the evolvement of the fire size, the spread of the burning area, the soot produced by different fuels and other hazardous fire productions. Besides, more critical events can be defined in these scenarios, including the density of the smoke and CO, the temperature and the level of the heat flux. Potential noises existing in the practical data should be considered by adding the noise into the training database. The AI model needs to be modified based on the requirement of predictions on these fire scenarios, parameters and critical events. The predicted results could be displayed on the digital twin, which would be a larger model for more complicated tunnels.

Large-scale fire tests. The proposed system has demonstrated its capability in monitoring the fire scenarios and give suggestions for firefighting in real-time. However, the real situations are more complicated since the tunnel and its environment may vary case by case. For instance, the shape and size of a tunnel may differ from those we assumed, and the information showing on the user interface should be altered depending on the requirement of the local department. Thus, large- or real-scale tunnel fire tests would be preferably conducted to further demonstrate the feasibility of the system before being applied in practice.

Linking with the sprinkler system. The firefighting system could be linked with the sprinkler system. The orientation of the sprinkler and the water faucet can be changed according to the fire location recognized by the AI model. This makes extinguishing more intelligent and efficient. The current sprinkler will be upgraded to satisfy the requirement of smart fire safety for tunnels.

The proposed system, which though has many imperfections, would be a good start to facilitate smart firefighting. The database, AI model and the user interface are continuously developed and publicly available on Github: https://github.com/PolyUFire/Tunnel_Fire_System. It is imaginable that the system will be more feasible and powerful with the contributions of more researchers.

6 Conclusions

In this study, a Smart Firefighting Digital Twin for tunnel fire is proposed and demonstrated on a small-scale tunnel. The system comprises four main components and can provide valuable information for supporting the firefighters to make decisions. The intelligence of the system is embodied by its AI engine, which is constructed with three LSTM layers and trained with a large numerical database. The proposed AI model attains an accuracy of 98% in predicting the fire source information on the database. The temperature distribution in the tunnel can also be visualized by matching the predicted fire scenario with the most likely case stored in the database. Without further tuning, the trained AI model can be applied on a small-scale tunnel (scale is 1:50) to recognize fire scenarios. The results show that compared with the size of the fire, the fire location is easier to be identified. By defining a critical event on the size of the fire, the trained AI model is enabled to give warnings to firefighters.

The total time delay is only around 1 s from the on-site measurement of temperature to displaying the predictions on a remote user interface, proving that the proposed system is quite swift and satisfactory. The system is also robust to give predictions even if a portion of thermocouples fail during fire incidents. This mainly benefits from the adoption of the filter algorithm for the input data of the AI model. Since real fire scenarios may be more complicated than expected, the proposed intelligent system may need further improvement before being applied in practice.

Acknowledgements

This work is funded by the Hong Kong Research Grants Council Theme-based Research Scheme (T22-505/19-N), National Natural Science Foundation of China (NSFC grant no. 52108480), the PolyU Emerging Frontier Area (EFA) Scheme of RISUD (P0013879) and Start-up Fund (P0036363). The authors also thank Yanfu Zeng (PolyU) for assisting the software development.

CRediT authorship contribution statement

Xiqiang Wu: Writing - original draft, Investigation, Methodology, Software, Formal analysis. **Xiaoning Zhang:** Investigation, Writing - original draft. **Yishuo Jiang:** Investigation, Resources. **Xinyan Huang**: Conceptualization, Supervision, Writing - review & editing, Funding acquisition. **George G.Q. Huang**: Resources, Supervision. **Asif Usmani**: Methodology, Funding acquisition, Supervision.

References

Adamowski J, Karapataki C (2010) Comparison of multivariate regression and artificial neural networks for peak urban water-demand forecasting: Evaluation of different ANN learning algorithms. *Journal of Hydrologic Engineering* **15**, 729–743.

Akhloufi MA, Booto Tokime R, Elassady H (2018) Wildland fires detection and segmentation using deep learning. In 'Proc. Vol. 10649, Pattern Recognit. Track. XXIX; 106490B', 11

Aksoy S, Haralick RM (2001) Feature normalization and likelihood-based similarity measures for image retrieval. *Pattern Recognition Letters* **22**, 563–582.

Alzubaidi L, Al-Shamma O, Fadhel MA, Farhan L, Zhang J (2020) Classification of red blood cells in sickle cell anemia using deep convolutional neural network. *Advances in Intelligent Systems and Computing* **940**, 550–559.

Aralt TT, Nilsen AR (2009) Automatic fire detection in road traffic tunnels. *Tunnelling and Underground Space Technology* **24**, 75–83.

Arora R, Basu A, Mianjy P, Mukherjee A (2018) Understanding deep neural networks with rectified linear units. *6th International Conference on Learning Representations, ICLR 2018 - Conference Track Proceedings* 1–17.

Baek J, Alhindi TJ, Jeong YS, Jeong MK, Seo S, Kang J, Shim W, Heo Y (2021) Real-time fire detection system based on dynamic time warping of multichannel sensor networks. *Fire Safety Journal* **123**, 103364.

Baum H, Mccaffrey B (1989) Fire Induced Flow Field - Theory And Experiment. *Fire Safety Science*

2, 129–148.

Beard AN (2009) Fire safety in tunnels. *Fire Safety Journal* **44**, 276–278.

Bermúdez JD, Achanccaray P, Sanches ID, Cue L, Happ P, Feitosa RQ (2017) EVALUATION OF RECURRENT NEURAL NETWORKS FOR CROP RECOGNITION FROM MULTITEMPORAL REMOTE SENSING IMAGES Rio de Janeiro State University , Brazil. 800–804.

Cao Y, Yang F, Tang Q, Lu X (2019) An attention enhanced bidirectional LSTM for early forest fire smoke recognition. *IEEE Access* **7**, 154732–154742.

Casey N (2020) Fire incident data for Australian road tunnels. *Fire Safety Journal* **111**, 102909.

Chen MY (2011) Predicting corporate financial distress based on integration of decision tree classification and logistic regression. *Expert Systems with Applications* **38**, 11261–11272.

Chen L, Mao P, Zhang Y, Xing S, Li T (2020) Experimental study on smoke characteristics of bifurcated tunnel fire. *Tunnelling and Underground Space Technology* **98**, 103295.

Cowlard A, Jahn W, Abecassis-Empis C, Rein G, Torero JL (2010) Sensor assisted fire fighting. *Fire Technology* **46**, 719–741.

Danziger NH, Kennedy WD (1982) Longitudinal ventilation analysis for the Glenwood Canyon tunnels. In 'Proc. 4th Int. Symp. Aerodyn. Vent. Veh. Tunnels',

Dexters A, Leisted RR, Van Coile R, Welch S, Jomaas G (2020) Testing for knowledge: Application of machine learning techniques for prediction of flashover in a 1/5 scale ISO 13784-1 enclosure. *Fire and Materials* 1–12.

Gaur A, Singh A, Kumar A, Kumar A, Kapoor K (2020) Video Flame and Smoke Based Fire Detection Algorithms: A Literature Review. *Fire Technology* **56**, 1943–1980.

Ghoreishi (2019) Review of the Punching Shear Behavior of Concrete Flat Slabs in Ambient and Elevated Temperature Mehrafarid. 8301–8305.

Govil K, Welch ML, Ball JT, Pennypacker CR (2020) Preliminary results from a wildfire detection system using deep learning on remote camera images. *Remote Sensing* **12**,.

Grant C, Hamins A, Bryner N, Jones A, Koepke G (2015) Research Roadmap for Smart Fire Fighting Summary Report Research Roadmap for.

Greff K, Srivastava RK, Koutnik J, Steunebrink BR, Schmidhuber J (2017) LSTM: A Search Space Odyssey. *IEEE Transactions on Neural Networks and Learning Systems* **28**, 2222–2232.

Haack A (2002) Current safety issues in traffic tunnels. *Tunnelling and Underground Space Technology* **17**, 117–127.

Han D, Lee B (2009) Flame and smoke detection method for early real-time detection of a tunnel fire. *Fire Safety Journal* **44**, 951–961.

Han L, Potter S, Beckett G, Pringle G, Welch S, Koo SH, Wickler G, Usmani A, Torero JL, Tate A (2010) FireGrid: An e-infrastructure for next-generation emergency response support. *Journal of Parallel and Distributed Computing* **70**, 1128–1141.

Hochreiter S (1997) Long Short-Term Memory. **1780**, 1735–1780.

Hodges JL, Lattimer BY (2019) Wildland Fire Spread Modeling Using Convolutional Neural Networks. *Fire Technology* **55**, 2115–2142.

Hurley MJ, Gottuk D, Hall JR, Harada K, Kuligowski E, Puchovsky M, Torero J, Watts JjM, Wieczorek C (2016) SFPE handbook of fire protection engineering, fifth edition. *SFPE Handbook of Fire*

Protection Engineering, Fifth Edition 1–3493.

Ingason H, Li YZ, Lönnermark A (2015) 'Tunnel fire dynamics.' (Springer: London)

Ingason H, Lönnermark A (2012) Heat release rates in tunnel fires: a summary. *Handbook of Tunnel Fire Safety* 309–328.

Jahn W, Rein G, Torero JL (2011) Forecasting fire growth using an inverse zone modelling approach. *Fire Safety Journal* **46**, 81–88.

Jahn W, Rein G, Torero JL (2012) Forecasting fire dynamics using inverse computational fluid dynamics and tangent linearisation. *Advances in Engineering Software* **47**, 114–126.

Jevtić RB, Blagojević MDJ (2014) On a linear fire detection using coaxial cables. *Thermal Science* **18**, 603–614.

Jiang S, Zhu S, Guo X, Chen C, Li Z (2020) Safety monitoring system of steel truss structures in fire. *Journal of Constructional Steel Research* **172**, 106216.

Kavzoglu T, Mather PM (2003) The use of backpropagating artificial neural networks in land cover classification. *International Journal of Remote Sensing* **24**, 4907–4938.

Koekkoek EJW, Booltink H (1999) Neural network models to predict soil water retention. *European Journal of Soil Science* **50**, 489–495.

Koffmane G, Hoff H (2010) More than just fire detection: fibre optic linear heat detection (DTS) enables fire monitoring in road-and rail-tunnels. In 'Proc. from Fourth Int. Symp. Tunn. Saf. Secur. Frankfurt am Main, Ger. March 17-19, 2010', 525

Komer B, Bergstra J, Eliasmith C (2014) Hyperopt-Sklearn: Automatic Hyperparameter Configuration for Scikit-Learn. *Proceedings of the 13th Python in Science Conference* 32–37.

Krogh JW, Krogh, Gennick (2018) 'MySQL Connector/Python Revealed.' (Springer)

Kumar J, Goomer R, Singh AK (2018) Long Short Term Memory Recurrent Neural Network (LSTM-RNN) Based Workload Forecasting Model for Cloud Datacenters. *Procedia Computer Science* **125**, 676–682.

Li YZ, Ingason H (2018) Overview of research on fire safety in underground road and railway tunnels. *Tunnelling and Underground Space Technology* **81**, 568–589.

Li YZ, Lei B, Ingason H (2013) Theoretical and experimental study of critical velocity for smoke control in a tunnel cross-passage. *Fire technology* **49**, 435–449.

Li J, Liu J (2020) Science Mapping of Tunnel Fires: A Scientometric Analysis-Based Study. *Fire Technology*.

Liu ZG, Kashef AH, Lougheed GD, Crampton GP (2011a) Investigation on the Performance of Fire Detection Systems for Tunnel Applications--Part 1: Full-Scale Experiments at a Laboratory Tunnel. *Fire Technology* **47**, 163–189.

Liu ZG, Kashef AH, Lougheed GD, Crampton GP (2011b) Investigation on the Performance of Fire Detection Systems for Tunnel Applications--Part 2: Full-Scale Experiments Under Longitudinal Airflow Conditions. *Fire Technology* **47**, 191–220.

Liu Z, Kim AK (2003) Review of recent developments in fire detection technologies. *Journal of Fire Protection Engineering* **13**, 129–151.

McGrattan K, Hostikka S, McDermott R, Floyd J, Weinschenk C, Overholt K (2017) FDS technical reference guide volume 1 : Mathematical Model.

Mcgrattan K, Mcdermott R (2015) Fire Dynamics Simulator User ' s Guide (FDS Version 6.3.0).

Morales G, Huam SG, Telles J (2018) 'Cloud Detection in High-Resolution Multispectral Satellite Imagery Using Deep Learning : 27th International Conference on Artificial Neural Networks , Cloud Detection in High-Resolution Multispectral Satellite Imagery Using Deep Learning.' (Springer International Publishing)

Ren R, Zhou H, Hu Z, He S, Wang X (2019) Statistical analysis of fire accidents in Chinese highway tunnels 2000–2016. *Tunnelling and Underground Space Technology*.

Sayad YO, Mousannif H, Al Moatassime H (2019) Predictive modeling of wildfires: A new dataset and machine learning approach. *Fire Safety Journal* **104**, 130–146.

Sharma A, Singh PK, Kumar Y (2020) An integrated fire detection system using IoT and image processing technique for smart cities. *Sustainable Cities and Society* **61**, 102332.

Sun M, Raju A, Tucker G, Panchapagesan S, Fu G, Mandal A, Matsoukas S, Strom N, Vitaladevuni S (2017) Max-pooling loss training of long short-term memory networks for small-footprint keyword spotting. *2016 IEEE Workshop on Spoken Language Technology, SLT 2016 - Proceedings* 474–480.

Wang J, Tam CW, Jia Y, Peacock R, Reneke P, Yujun E, Cleary T (2021) P-Flash – A machine learning-based model for flashover prediction using recovered temperature data. *Fire Safety Journal* **122**, 103341.

Wu Y, Liu Y, Li J, Liu H, Hu X (2013) Traffic sign detection based on convolutional neural networks. *Proceedings of the International Joint Conference on Neural Networks*.

Wu X, Park Y, Li A, Huang X, Xiao F, Usmani A (2020) Smart Detection of Fire Source in Tunnel Based on the Numerical Database and Artificial Intelligence. *Fire Technology*.

Wu X, Zhang X, Huang X, Xiao F, Usmani A, Xiqiang, Wu, Xiaoning, Zhang, Xinyan, Huang, Fu, Xiao, Usmani A (2021) A real-time forecast of tunnel fire based on numerical database and artificial intelligence. *Building Simulation*.

Yang Z, Wang T, Bu L, Ouyang J (2021) Training with Augmented Data: GAN-based Flame-Burning Image Synthesis for Fire Segmentation in Warehouse. *Fire Technology*.

Zhai C, Zhang S, Cao Z, Wang X (2020) Learning-based prediction of wildfire spread with real-time rate of spread measurement. *Combustion and Flame* **215**, 333–341.

Zhang X, Wu X, Park Y, Zhang T, Huang X, Xiao F, Usmani A (2021) Perspectives of big experimental database and artificial intelligence in tunnel fire research. *Tunnelling and Underground Space Technology* **108**, 103691.

Zone M (1997) MySQL 5.0 Reference Manual. *Consultado del día* **13**,.